doi: 10.13241/j.cnki.pmb.2019.10.013

·临床研究·

磁共振扩散加权成像对宫颈癌诊断价值及其与临床病理特征的关系研究 *

杨 皓 吴勘华 宋 恬 孙荣跃 殷士蒙△

（复旦大学附属华东医院放射科 上海 200040）

摘要 目的:研究磁共振扩散加权成像(DWI)对宫颈癌的诊断价值及其与临床病理特征的关系。**方法:**将 2016 年 5 月至 2018 年 5 月间于本院接受诊治的 90 例宫颈癌患者作为研究组,其中鳞癌 69 例,腺癌 21 例。另选择同期因其他原因来本院行宫颈检查的 90 例非宫颈癌患者作为对照组,两组患者均接受常规磁共振成像(MRI)平扫及 DWI 检查。观察两组 MRI 影像学特征,分别比较研究组和对照组、不同病理分型以及不同临床病理特征宫颈癌患者表观弥散系数(ADC)值,采用受试者工作特征(ROC)曲线评价 DWI 检查对宫颈癌的诊断价值,并分析宫颈癌患者 ADC 值与临床病理特征的关系。**结果:**研究组和对照组的 MRI 影像学图像全部符合诊断和测量要求,无显著的伪影、变形;研究组患者的病变位在宫颈,其信号特征 T1 加权像(T1WI)显示为等信号,而 T2 加权像(T2WI)显示为稍高 / 高信号,经 DWI 检查显示为高信号肿块,且边界清晰。研究组患者 DWI 检查的 ADC 值低于对照组(*P<0.05*);鳞癌患者 DWI 检查的 ADC 值也明显低于腺癌患者(*P<0.05*)。ROC 曲线结果显示,DWI 检查鉴别诊断宫颈癌和非宫颈癌、鳞癌和腺癌的 AUC 分别为 0.912、0.827。无淋巴结转移、临床病理分期为Ⅰ-Ⅱ期、中 / 高分化以及肿瘤细胞间质占比＜70%的宫颈癌患者 ADC 值分别高于有淋巴结转移、临床病理分期为Ⅲ-Ⅵ期、低分化以及肿瘤细胞间质占比≥ 70%的宫颈癌患者(均 *P<0.05*)。**结论:**DWI 对宫颈癌诊断价值高,且 DWI 成像参数 ADC 值和宫颈癌的部分临床病理特征关系密切,能从一定程度上辅助医师了解宫颈癌病理分型、病理分期、分化程度及有无淋巴结转移。

关键词:磁共振扩散加权成像;宫颈癌;诊断价值;临床病理特征

中图分类号:R737.33;R445.2 **文献标识码:**A **文章编号:**1673-6273(2019)10-1870-05

Diagnostic Value of Magnetic Resonance Diffusion-weighted Imaging in Cervical Cancer and Its Relationship with Clinicopathological Features*

YANG Hao, WU Kan-hua, SONG Tian, SUN Rong-yue, YIN Shi-meng△

(Department of Radiology, Huadong Hospital Affiliated to Fudan University, Shanghai, 200040, China)

ABSTRACT Objective: To study the diagnostic value of magnetic resonance diffusion-weighted imaging (DWI) in cervical cancer and its relationship with clinicopathological features. **Methods:** 90 cases of patients with cervical cancer who were treated in our hospital from May 2016 to May 2018 were enrolled as the study group. There were 69 cases of squamous cell carcinoma and 21 cases of adenocarcinoma. Another 90 patients without cervical cancer who underwent cervical examination for other reasons were selected as the control group. The two groups of patients underwent conventional magnetic resonance imaging (MRI) plain scan and DWI examination. The MRI imaging features of the two groups were observed. Apparent diffusion coefficient (ADC) values were compared between the study group and the control group, different pathological types and clinicopathological features of cervical cancer patients. Receiver operating characteristic (ROC) curve was used to evaluate the diagnostic value of DWI in cervical cancer. The relationship between ADC value and clinicopathological features of cervical cancer patients was analyzed. **Results:** MRI images of the study group and the control group all met the requirements of diagnosis and measurement, without significant artifacts and distortion. The lesions in the study group were located in the cervix, and their signal characteristics T1 weighted imaging (T1WI) showed equal signal. T2-weighted imaging (T2WI) showed slightly high/high signal, and DWI showed a high signal mass, and the boundary was clear. The ADC value of DWI in the study group was lower than that in the control group (*P<0.05*). The ADC value of DWI in squamous cell carcinoma patients was also significantly lower than that in adenocarcinoma patients (*P<0.05*). The ROC curve showed that the AUC of DWI in examination for differential diagnosis of cervical cancer and non cervical cancer, squamous cell carcinoma and adenocarcinoma were 0.912 and 0.827 respectively. The ADC values of cervical cancer patients with no lymph node metastasis, stage I-II, medium/high differentiation and intercellular proportion of tumor cells＜70% were higher than those of cervical cancer patients with lymph node metastasis, stage III-VI,

* 基金项目:上海市卫生和计划生育委员会科研项目(2016Y1036)

作者简介:杨皓(1976-),男,本科,主治医师,从事医学影像诊断及介入治疗方面的研究,E-mail: plpiav@163.com

△ 通讯作者:殷士蒙(1965-),男,本科,副主任医师,从事医学影像诊断及介入治疗方面的研究,E-mail: vrtmm3@163.com

(收稿日期:2018-10-12 接受日期:2018-10-31)

poorly differentiation and intercellular proportion of tumor cells≥ 70% (*P<0.05*). **Conclusion:** DWI has a high diagnostic value for cervical cancer. DWI imaging parameters ADC value is closely related to the clinicopathological features of cervical cancer. To some extent, it can help doctors to understand the pathological classification, clinicopathological stage, degree of differentiation and lymph node metastasis of cervical cancer.

Key words: Magnetic resonance diffusion-weighted imaging;Cervical cancer; Diagnostic value; Clinicopathological features

Chinese Library Classification(CLC): R737.33; R445.2 Document code: A

Article ID: 1673-6273(2019)10-1870-05

前言

宫颈癌作为女性生殖系统高发性恶性肿瘤,其发病率仅低于乳腺癌,且发病越来越趋于年轻化[1,2]。研究发现,宫颈癌发病早期较为隐匿,缺乏显著的临床表现,造成临床早期检出率较低,一些患者在入院确诊时已发展至中晚期,进而错过了最佳手术治疗时机,故积极寻找安全、高效的早期诊断方式至关重要[3,4]。磁共振成像(Magnetic resonance imaging, MRI)作为临床诊断宫颈癌常用的无创影像学方法,能多方位成像,便于临床准确了解肿瘤的浸润深度、体积等情况[5,6]。而磁共振扩散加权成像(Diffusion weighted imaging, DWI)作为临床筛查癌变的新型影像学手段,其可以在活体上实施水分子扩散测量,能够反映活体组织形态以及活体的具体组织功能状态,具有操作简便、准确性高及无创等优势[7,8]。本研究通过分析 DWI 对宫颈癌的诊断价值以及其与病理特征的关系,以期为临床合理制定诊治方案提供依据,报道如下。

1 资料与方法

1.1 一般资料

将 2016 年 5 月至 2018 年 5 月期间于本院接受诊治的 90 例宫颈癌患者作为研究组,纳入标准:(1)入选患者均通过组织病理学检查确诊为宫颈癌;(2)研究前未经手术及放疗、化疗等治疗者;(3)无血液系统疾病、传染性疾病、神经系统疾病、自身免疫系统疾病及其他恶性肿瘤。排除标准:(1)存在严重的心、肺、肝、肾等相关脏器功能疾病者;(2)妊娠期、哺乳期女性;(3)预计生存期较短,不能完成本研究者。所有患者年龄 37-76 岁,平均(57.13± 4.22)岁;体质量指数(Body mass index, BMI) 20.02-24.15 kg/m^2,平均(22.44± 0.53)kg/m^2;病理分型:69 例为鳞癌,21 例为腺癌;其中 20 例有淋巴结转移,70 例无淋巴结转移;临床病理分期:51 例为Ⅰ-Ⅱ期,39 例为Ⅲ-Ⅵ期;分化程度:47 例为中/高分化,43 例为低分化;肿瘤细胞间质占比:36 例<70%,54 例≥ 70%。另选取同期因其他原因来本院行宫颈检查的 90 例非宫颈癌患者作为对照组,年龄 35-78 岁,平均(56.09± 4.37)岁;BMI 20.75-24.18 kg/m^2,平均(22.46± 0.28) kg/m^2;盆部下坠痛 20 例,白带增多 30 例,阴道不规则流血 15 例,接触性阴道出血 25 例。

两组受试者的年龄、BMI 分布比较无差异(*P>0.05*),本研究符合我院伦理学要求,所有患者与家属对本研究全部知情且签署同意书。

1.2 方法

1.2.1 MRI **检查** 患者均于非月经期接受检查,如存在宫内节育器者,在检查前将其取出;告知两组患者于检查前 60 min 摄入 500 mL 左右水,以使膀胱适当充盈。选择 GE 1.5T signa excite 超导型 MRI(生产厂商:美国通用电气公司)实施检查,取仰卧位,开展常规的 MRI 检查。MRI 各参数设置为:① 轴位 T1WI 参数设置:层间距设定为 1 mm,层厚设定为 6mm,重复时间(Repetition Time,TR)设定成 600 ms,回波时间(EchedelayTime, TE)设定成 7.4 ms,将矩阵设定成 224× 320,而视野(field of view, FOV)设定为 36 cm× 36 cm;② T2WI、T2 脂肪抑制序列:层间距设定为 1 mm,层厚设定为 6 mm,TR 设定为 3820 ms,TE 设定为 87.5 ms,将矩阵设定在 224× 320,而 FOV 设定为 36 cm× 36 cm;扫描范围为由耻骨联合下缘至患者的腹部主动脉分叉处。

1.2.2 DWI **检查** 指导患者胸式呼吸,确保呼吸均匀,选择 SE-EPI(自旋回波 - 平面回波)序列,选择 MRI 扫描中 STIR 序列(脂肪抑制序列短时间反转恢复序列)实施脂肪压脂,将层厚设定为 5 mm,TR 设定为 7500 ms,TE 设定为 68 ms,层间隔为 0.5 mm,矩阵设定成 192× 144,而 FOV 设定为 385 cm× 385 cm,层数为 30 层,b 值选择 0 s/mm^2、800 s/mm^2,控制时间 180 s。

1.2.3 **图像处理** 将常规 MRI 检查、DWI 检查获得的图像资料上传到系统匹配的 AW4.4 工作站实施处理,排除产生的伪影,选择盆腔各器官组织对比清晰、分辨率高的图像,在工作站通过对 DWI 检查数据进行处理操作,得到相应的表观弥散系数(Apparent diffusion coefficient, ADC)值。

1.2.4 **采集病理组织标本** 经手术切除研究组患者的肿瘤并获取标本,选择肿瘤均质部分,尽量和 DWI 上相关感兴趣区域维持一致,分析切片组织学特点,确保每张切片经 2 名经验丰富的影像学医师独立阅片、协商获得判定结果。

1.3 观察指标

观察两组患者的 MRI 影像学特征,分别比较研究组和对照组、不同病理分型以及不同临床病理特征宫颈癌患者的 ADC 值,采用受试者工作特征(Receiver operating characteristics,ROC)曲线评价 DWI 检查对宫颈癌的诊断价值,并分析宫颈癌患者 ADC 值与临床病理特征的关系。

1.4 统计学方法

选择 SPSS 20.0 软件进行统计分析。计量资料应用($\bar{x}\pm s$)表示,行 t 检验。计数资料用 n(%)表示,行 χ^2 检验。采用 ROC 曲线分析 DWI 诊断宫颈癌的诊断价值。*P<0.05* 代表差异有统计学意义。

2 结果

2.1 MRI 影像学特征

两组患者的 MRI 影像学图像全部符合诊断和测量要求,无显著的伪影、变形;研究组患者的病变位在宫颈,其信号特征

T1WI 显示为等信号;而 T2WI 显示为稍高 / 高信号;经 DWI 检查显示为高信号肿块,且边界清晰。

2.2 研究组与对照组以及不同病理分型宫颈癌患者 ADC 值比较

研究组患者 DWI 检查的 ADC 值低于对照组(*P<0.05*);鳞癌患者 DWI 检查的 ADC 值也明显低于腺癌患者(*P<0.05*)。详见表 1。

表 1 研究组与对照组以及不同病理分型宫颈癌患者 ADC 值比较

Table 1 Comparison of ADC values between the study group and the control group and patients with different pathological types of cervical cancer

Groups	n	ADC value($10^{-3}mm^2/s$)	Pathological types	n	ADC value($10^{-3}mm^2/s$)
Control group	90	1.42± 0.31	Squamous cell carcinoma	69	0.76± 0.26
Study group	90	0.81± 0.22	Adenocarcinoma	21	0.97± 0.14
t		15.224			4.801
P		0.000			0.000

2.3 DWI 对宫颈癌诊断价值

以本研究中对照组(非宫颈癌)和研究组(宫颈癌)资料为样本,进行 ROC 分析。结果:ROC 曲线鉴别诊断宫颈癌和非宫颈癌的 AUC 为 0.912,95%CI 为 0.817-1.000,灵敏度、特异度分别为 88.56%、86.80%,最佳的 ADC 阈值是 1.10× 10^{-3} mm^2/s;详见图 1(A)。

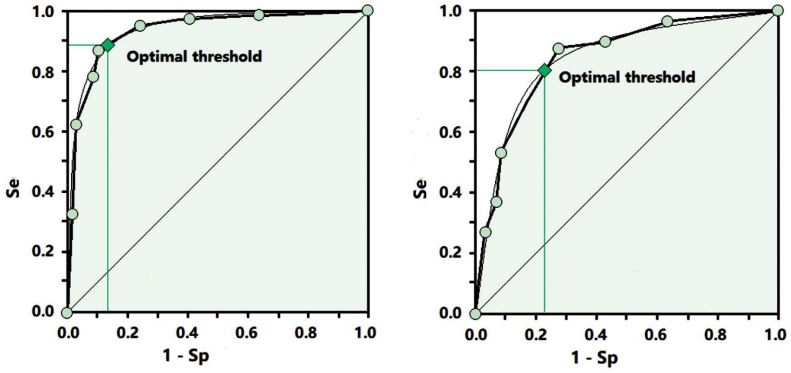

(A) (B)

图 1 DWI 对宫颈癌诊断价值的 ROC 分析曲线

Fig.1 ROC analysis of diagnostic value of DWI for cervical cancer

注:A 为鉴别诊断宫颈癌和非宫颈癌的 ROC 分析曲线;B 为鉴别诊断鳞癌和腺癌的 ROC 分析曲线

Note: A is a ROC analysis curve for differential diagnosis of cervical cancer and non cervical cancer; B is a ROC analysis curve for differential diagnosis of squamous cell carcinoma and adenocarcinoma.

以本研究中研究组(宫颈癌,其中鳞癌患者 69 例,腺癌患者 21 例)资料为样本,进行 ROC 分析。结果:ROC 曲线鉴别诊断鳞癌和腺癌的 AUC 为 0.827,95%CI 为 0.743-0.911,灵敏度、特异度分别为 80.62%、76.71%,最佳的 ADC 阈值是 0.94× 10^{-3} mm^2/s;详见图 1(B)。

2.4 不同病理特征宫颈癌患者的 ADC 值比较

无淋巴结转移、临床病理分期为Ⅰ-Ⅱ期、中 / 高分化以及肿瘤细胞间质占比<70%的宫颈癌患者 ADC 值分别高于有淋巴结转移、临床病理分期为Ⅲ-Ⅵ期、低分化以及肿瘤细胞间质占比≥ 70%的宫颈癌患者(均 *P<0.05*);详见表 2。

表 2 不同病理特征宫颈癌患者的 ADC 值比较 ($\bar{x}\pm s$)

Table 2 Comparison of ADC values of cervical cancer patients with different pathological features($\bar{x}\pm s$)

Clinicopathological features		n	ADC value(× 10^{-3} mm^2/s)	t	*P*
Lymph node metastasis	Yes	20	0.55± 0.21	5.449	5.449
	No	70	0.88± 0.32		
Clinicopathological stage	Ⅰ-Ⅱ stage	51	0.91± 0.21	5.044	0.000
	Ⅲ-Ⅵ stage	39	0.68± 0.22		
Degree of differentiation	Medium / high differentiation	47	0.98± 0.31	6.119	0.000
	Poorly differentiation	43	0.62± 0.24		
Intercellular proportion of tumor cells	<70%	36	0.93± 0.12	5.068	0.000
	≥ 70%	54	0.73± 0.25		

3 讨论

宫颈癌是一种常见的女性疾病,好发于 30-45 岁群体。随着人们生活习惯的改变,宫颈癌发病率呈升高趋势,且呈年轻化[9]。MRI 虽然可以很好的显示软组织形态结构,但对纤维瘢痕组织、小体积复发肿瘤病灶和血管的显示效果不佳,也不能显示器官的功能状态,可能存在漏诊 [10-12]。而 DWI 作为新型 MRI 成像技术,其和常规的 MRI 存在一定差异,DWI 主要可以通过组织内水分子的弥散状态来反映待测组织的生理功能和病理状态[13-15]。ADC 值是在 DWI 检查中反映组织情况相关弥散特征的主要参数,其可衡量水分子在人体组织环境中的弥散运动,对组织内水分子具体弥散状态可进行突出显示,从而能反映病变组织学状况。

本研究结果显示,研究组与对照组患者的 MRI 影像学图像全部符合诊断、测量要求,无显著的伪影、变形;研究组患者的病变位在宫颈,其信号特征 T1WI 显示为等信号,而 T2WI 显示为稍高 / 高信号,经 DWI 检查显示为高信号肿块,且边界清晰。提示 DWI 检查可对宫颈癌的具体状况进行突出显示,使宫颈癌和周围结构之间产生明显对比,便于临床诊断判定癌变[16-18]。MRI 是通过多参数、多方位呈现反映宫颈癌的形态学特征,对功能成像体征反映较差。而 DWI 是一种兼有功能性检查的诊断方法,其经多序列、多参数、多方位成像,可以有效评估宫颈癌的病变形态学特征及功能成像体征,使临床鉴别诊断准确性提高。本研究结果还发现,相较于对照组,研究组患者的 ADC 值降低;而相较于鳞癌组患者,腺癌组患者的 ADC 值升高;且经 ROC 曲线分析发现,DWI 检查对鉴别诊断宫颈癌和非宫颈癌、鳞癌和腺癌存在较高诊断效能。提示实施 DWI 检查可以辅助临床医师鉴别诊断宫颈癌,了解宫颈癌的病理分型[19-21]。同时,无淋巴结转移、临床病理分期Ⅰ-Ⅱ期、中 / 高分化、肿瘤细胞间质占比＜70%的宫颈癌患者 ADC 值高于有淋巴结转移、临床病理分期Ⅲ-Ⅵ期、低分化、肿瘤细胞间质占比≥ 70%患者。提示 DWI 成像参数 ADC 值和宫颈癌患者的临床病理特征存在相关性[22,23]。ADC 值可对水分子的扩散运动能力强弱进行定量反映 [24]。目前研究发现肿瘤组织与机体正常组织结构有很大区别,肿瘤细胞密度升高可以显著限制水分子的活动,导致 ADC 值降低[25-27];同时肿瘤细胞中可溶性的大分子细胞骨架及纤维基质、细胞器对细胞中水分子的扩散运动均存在影响,亦可造成 ADC 值下降[28-30]。因此不同肿瘤组织 ADC 含有水分不同,在进行扫描时可以反映肿瘤淋巴结转移、临床病理分期、肿瘤分化程度、肿瘤细胞间质情况。

综上所述,DWI 在诊断宫颈癌方面应用价值较高,DWI 成像参数 ADC 值和宫颈癌的淋巴结转移、临床病理分期、分化程度、肿瘤细胞间质占比存在相关性,能从一定程度上辅助医师对宫颈癌诊治提供信息,值得临床推广。

参 考 文 献(References)

[1] US Preventive Services Task Force, Curry SJ, Krist AH, et al. Screening for Cervical Cancer: US Preventive Services Task Force Recommendation Statement[J]. JAMA, 2018, 320(7): 674-686

[2] 陈舒,罗新,帅翰林,等.宫颈癌组织中的 PTEN, VEGF 和 CD105 的表达及临床意义[J]. 现代生物医学进展, 2017, 17(9): 1696-1699

[3] Onal C, Yildirim BA, Guler OC, et al. The Utility of Pretreatment and Posttreatment Lymphopenia in Cervical Squamous Cell Carcinoma Patients Treated With Definitive Chemoradiotherapy[J]. Int J Gynecol Cancer, 2018, 28(8): 1553-1559

[4] Ronco G, Dillner J, Elfström KM, et al. Efficacy of HPV-based screening for prevention of invasive cervical cancer: follow-up of fourEuropean randomised controlled trials [J]. Lancet, 2014, 383 (9916): 524-532

[5] Agoston-Coldea L, Lupu S, Mocan T. Pulmonary Artery Stiffness by Cardiac Magnetic Resonance Imaging Predicts Major Adverse Cardiovascular Events in patients with Chronic Obstructive Pulmonary Disease[J]. Sci Rep, 2018, 8(1): 14447

[6] Yildirim N, Saatli B, Kose S, et al. Predictability of myometrial, lower uterine segment and cervical invasion with 3D transvaginal ultrasonography and magnetic resonance imaging in endometrial cancer patients: a prospective cohort study[J]. Med Ultrason, 2018, 20 (3):348-354

[7] Ueno YR, Tamada T, Takahashi S, et al. Computed Diffusion-Weighted Imaging in Prostate Cancer: Basics, Advantages, Cautions, and Future Prospects[J]. Korean J Radiol, 2018, 19(5): 832-837

[8] Luczyńska E, Heinze-Paluchowska S, Domalik A, et al. The Utility of Diffusion Weighted Imaging (DWI) Using Apparent Diffusion Coefficient (ADC) Values in Discriminating Between Prostate Cancer and Normal Tissue[J]. Pol J Radiol, 2014, 79(1): 450-455

[9] Weiss D, Koopmann M, Stenner M, et al. Clinicopathological characteristics of carcinoma from unknown primary in cervical lymph nodes[J]. Eur Arch Otorhinolaryngol, 2015, 272(2): 431-437

[10] Mittal P, Chopra S, Pant S, et al. Standard Chemoradiation and Conventional Brachytherapy for Locally Advanced Cervical Cancer: Is It Still Applicable in the Era of Magnetic Resonance-Based Brachytherapy?[J]. J Glob Oncol, 2018, 37(4): 1-9

[11] Chen XL, Chen GW, Xu GH, et al. Tumor Size at Magnetic Resonance Imaging Association With Lymph Node Metastasis and Lymphovascular Space Invasion in Resectable Cervical Cancer: A Multicenter Evaluation of Surgical Specimens [J]. Int J Gynecol Cancer, 2018, 28(8): 1545-1552

[12] Zhang Z, Wang Z, Zhao R. Dynamic Contrast-Enhanced Magnetic Resonance Imaging of Advanced Cervical Carcinoma: The Advantage of Perfusion Parameters From the Peripheral Region in Predicting the Early Response to Radiotherapy [J]. Int J Gynecol Cancer, 2018, 28 (7): 1342-1349

[13] Qu JR, Qin L, Li X, et al. Predicting Parametrial Invasion in Cervical Carcinoma (Stages IB1, IB2, and IIA): Diagnostic Accuracy of T2-Weighted Imaging Combined With DWI at 3T [J]. AJR Am J Roentgenol, 2018, 210(3): 677-684

[14] Li X, Wang L, Li Y, et al. The Value of Diffusion-Weighted Imaging in Combination With Conventional Magnetic Resonance Imaging for Improving Tumor Detection for Early Cervical Carcinoma Treated With Fertility-Sparing Surgery[J]. Int J Gynecol Cancer, 2017, 27(8): 1761-1768

[15] Lin M, Yu X, Chen Y, et al. Contribution of mono-exponential, bi-exponential and stretched exponential model-based diffusion-weighted MR imaging in the diagnosis and differentiation of uterine

cervical carcinoma[J]. Eur Radiol, 2017, 27(6): 2400-2410

[16] Baron CA, Kate M, Gioia L, et al. Reduction of Diffusion-Weighted Imaging Contrast of Acute Ischemic Stroke at Short Diffusion Times [J]. Stroke, 2015, 46(8): 2136-2141

[17] Chavhan GB, Alsabban Z, Babyn PS. Diffusion-weighted imaging in pediatric body MR imaging: principles, technique, and emerging applications[J]. Radiographics, 2014, 34(3): 73-88

[18] Ichikawa S, Motosugi U, Morisaka H, et al. MRI-based staging of hepatic fibrosis: Comparison of intravoxel incoherent motion diffusion-weighted imaging with magnetic resonance elastography[J]. J Magn Reson Imaging, 2015, 42(1): 204-210

[19] Seo H, Choi J, Oh C, et al. Isotropic diffusion weighting for measurement of a high-resolution apparent diffusion coefficientmap using a single radial scan in MRI [J]. Phys Med Biol, 2014, 59(20): 6289-6303

[20] 张娜,王维青,武霞.MRI 最小 ADC 值取代平均 ADC 值在宫颈癌诊断及分期中的应用研究[J].医学影像学杂志, 2017, 27(9): 1774-1777

[21] Liu K, Ma Z, Feng L. Apparent diffusion coefficient as an effective index for the therapeutic efficiency of brain chemoradiotherapy for brain metastases from lung cancer [J]. BMC Med Imaging, 2018, 18 (1): 30

[22] LS Beltran, M Samim, S Gyftopoulos, et al. Does the Addition of DWI to Fluid-Sensitive Conventional MRI of the Sacroiliac Joints Improve the Diagnosis of Sacroiliitis? [J]. AJR Am J Roentgenol, 2018, 210(6): 1309-1316

[23] SG Kafali, T Kukur, EU Saritas. Phase-correcting non-local means filtering for diffusion-weighted imaging of the spinal cord [J]. Magnetic resonance in medicine, 2018, 80(3): 1020-1035

[24] Tsukasa Yoshida, Atsushi Urikura, Kensei Shirata, et al. Short tau inversion recovery in breast diffusion-weighted imaging: signal-to-noise ratio and apparent diffusion coefficients using a breast phantom in comparison with spectral attenuated inversion recovery [J]. La Radiologia medica, 2018, 123(4): 296-304

[25] CC Obele, C Glielmi, JReam, et al. Simultaneous Multislice Accelerated Free-Breathing Diffusion-Weighted Imaging of the Liver at 3T[J]. Abdominal imaging, 2015, 40(7): 2323-2330

[26] Anke Wouters, Bastian Cheng, Soren Christensen, et al. Automated DWI analysis can identify patients within the thrombolysis time window of 4.5 hours[J]. Neurology, 2018, 90(18): 1570-1577

[27] Masanori Ozaki, Yusuke Inoue, Tosiaki Miyati, et al. Motion artifact reduction of diffusion-weighted MRI of the liver: use of velocity-compensated diffusion gradients combined with tetrahedral gradients [J]. Journal of magnetic resonance imaging: JMRI, 2013, 37 (1): 172-178

[28] Chen L, Zhang J, Chen Y, et al. Relationship between apparent diffusion coefficient and tumour cellularity in lung cancer [J]. PLoS One, 2014, 9(6): e99865

[29] Bickel H, Pinker-Domenig K, Bogner W, et al. Quantitative apparent diffusion coefficient as a noninvasive imaging biomarker for the differentiation of invasive breast cancer and ductal carcinoma in situ [J]. Invest Radiol, 2015, 50(2): 95-100

[30] 肖胜,郭涛.磁共振扩散张量成像在评价以及神经根病变中的作用[J].中国 CT 和 MRI 杂志, 2016, 14(3): 51-54

(上接第 1863 页)

[17] Chen N, Feng L, Qu H, et al. Overexpression of IL-9 induced by STAT3 phosphorylation is mediated by miR-155 and miR-21 in chronic lymphocytic leukemia[J]. Oncol Rep, 2018, 39(6): 3064-3072

[18] Martin EC, Krebs AE, Burks HE, et al. miR-155 induced transcriptome changes in the MCF-7 breast cancer cell line leads to enhanced mitogen activated protein kinase signaling [J]. Genes Cancer, 2014, 5(9-10): 353-364

[19] Qu Ya-jing, Zhang Hai-yang, Sun Wu, et al. MicroRNA-155 promotes gastric cancer growth and invasion by negatively regulating transforming growth factor-β receptor 2[J]. Cancer Sci, 2018, 109(3): 618-628

[20] Wang L, Tang B, Han H, et al. miR-155 Affects Osteosarcoma MG-63 Cell Autophagy Induced by Adriamycin Through Regulating PTEN-PI3K/AKT/mTOR Signaling Pathway [J]. Cancer Biother Radiopharm, 2018, 33(1): 32-38

[21] Bartel DP: MicroRNAs: genomics, biogenesis, mechanism, and function[J]. Cell, 2004, 116: 281-297

[22] Starr R, Willson TA, Viney EM, et al. A family of cytokine-inducible inhibitors of signaling[J]. Nature, 1997, 387(6636): 917-921

[23] Culig Z. Suppressors of cytokine signalling-3 and -1 in human carcinogenesis[J]. Front Biosci (Schol Ed), 2013, 5: 277-283

[24] Elliott J, Hookham MB, Johnston JA. The suppressors of cytokine signalling E3 ligases behave as tumour suppressors [J]. Biochem Soc Trans, 2008, 36(3): 464-468

[25] Aigner P, Just V, Stoiber D. STAT3 isoforms: Alternative fates in cancer?[J]. Cytokine, 2018, pii: S1043-4666(18)30300-4

[26] Arora L, Kumar AP, Arfuso F, et al. The Role of Signal Transducer and Activator of Transcription 3 (STAT3) and Its Targeted Inhibition in Hematological Malignancies[J]. Cancers (Basel), 2018, 10(9)

[27] Morikawa T, Baba Y, Yamauchi M, et al. STAT-3 expression, molecular features, inflammation patterns, and prognosis in a database of 724 colorectal cancers [J]. Clin Cancer Res, 2011, 17(6): 1452-1462

[28] Huang C, Li H, Wu W, et al. Regulation of miR-155 affects pancreatic cancer cell invasiveness and migration by modulating the STAT3 signaling pathway through SOCS1 [J]. Oncol Rep, 2013, 30 (3): 1223-1230

[29] Lei K, Du W, Lin S, et al. 3B, a novel photosensitizer, inhibits glycolysis and inflammation via miR-155-5p and breaks the JAK/STAT3/SOCS1 feedback loop in human breast cancer cells [J]. Biomed Pharmacother, 2016, 82: 141-150

[30] Zhou X, Yan T, Huang C, et al. Melanoma cell-secreted exosomal miR-155-5p induce proangiogenic switch of cancer-associated fibroblasts via SOCS1/JAK2/STAT3 signaling pathway[J]. J Exp Clin Cancer Res, 2018, 37(1): 242